Coherent feedforward regulation of gene expression by *Caulobacter* σ^T and GsrN during hyperosmotic stress

Matthew Z. Tien, Benjamin J. Stein, Sean Crosson*

Department of Biochemistry and Molecular Biology, University of Chicago, Chicago, IL 60637. USA.

* Corresponding Author

E-mail: scrosson@uchicago.edu

Running title: *Caulobacter* regulatory response to hyperosmotic stress

Abstract

GsrN is a conserved small RNA that is under the transcriptional control of the general stress response (GSR) sigma factor, σ^T, and functions as a major post-transcriptional regulator of *Caulobacter crescentus* survival across multiple stress conditions. We have conducted molecular genetic studies aimed at defining features of GsrN structure that determine cell survival under hyperosmotic stress, and have applied biochemical, transcriptomic and proteomic methods to define molecular regulatory targets of GsrN under hyperosmotic conditions. The 5' end of GsrN, which includes a conserved cytosine-rich stem loop structure, is necessary for cell survival upon osmotic upshock. GsrN both activates and represses gene expression when cells encounter a hyperosmotic environment. Among the genes most highly activated by GsrN is an uncharacterized open reading frame we have named *osrP*, which is predicted to encode a 37 kDa glycine-zipper protein. We present evidence that GsrN physically interacts with *osrP* mRNA through its 5' C-rich stem loop to enhance OsrP protein expression. Given that σ^T directly activates *gsrN* and *osrP* transcription, and that GsrN post-transcriptionally activates OsrP protein expression, we conclude that *sigT*, *gsrN*, and *osrP* comprise a coherent feedforward loop. This study delineates transcriptional and post-transcriptional layers of *Caulobacter* gene expression control during hyperosmotic stress, uncovers a new regulatory target of GsrN, and defines a coherent feedforward motif within the *Caulobacter* GSR regulatory network.

Importance

Bacteria inhabit diverse niches, and must adapt their physiology to constant environmental fluctuations. A major response to environmental perturbation is to change gene expression. *Caulobacter* and other alphaproteobacteria initiate a complex gene expression program known as the general stress response (GSR) under conditions including oxidative stress, osmotic stress, and nutrient limitation. The GSR enables cell survival in these environments. Understanding how bacteria survive stress requires that we dissect gene expression responses, such as the GSR, at the molecular level. This study is significant as it defines transcriptional and post-transcriptional layers of

gene expression regulation in response to hyperosmotic stress. We further provide evidence that coherent feedforward motifs influence the system properties of the *Caulobacter* GSR pathway.

Introduction

Cells alter gene expression to adapt to environmental perturbations. In bacteria, two major mechanisms controlling transcription are two-component signaling (TCS) (1) and alternative sigma (σ) factor regulation (2, 3). In species of the class Alphaproteobacteria, crosstalk between these mechanisms is uniquely achieved via the protein, PhyR, which contains both a σ-like domain and a TCS receiver domain (4-7). Under a range of specific stress conditions, PhyR becomes phosphorylated and, through a protein partner switching mechanism (5), activates a gene expression program known as the general stress response (GSR). The GSR is required for survival under diverse environmental conditions (8, 9).

We recently developed a network-based algorithm (10) to interrogate publicly available gene expression datasets to predict genes functioning in stress survival in the alphaproteobacterium, *Caulobacter crescentus*. This led to the discovery of a conserved small RNA (sRNA), GsrN, that plays an important role in survival across distinct environmental conditions including hyperosmotic and oxidative stress (11). GsrN is directly activated by the GSR alternative sigma factor, σ^T, and imposes a post-transcriptional layer of gene expression regulation during the general stress response. In the case of hydrogen peroxide stress, GsrN protects cells by base pairing with the 5' leader sequence of *katG* mRNA to promote expression of KatG catalase/peroxidase protein (11). To date, the identity of genes regulated by GsrN under hyperosmotic stress conditions remain undefined. The goal of this study was to define structural features of *Caulobacter* GsrN that are required for hyperosmotic stress survival and to identify direct molecular targets of GsrN under hyperosmotic conditions.

The induction of sRNA expression by osmotic stress has been described in a handful of bacterial species (12-15). Examples of sRNAs with known roles in osmoregulation of gene expression include OmrA/OmrB (16), MicF (12), and MicC (17) in *Escherichia coli*. The OmrA/OmrB system is upregulated during osmotic stress by the two-component system, EnvZ-OmpR. OmrA/OmrB function as post-transcriptional feedback repressors of OmpR (18) and repress the expression of outer

membrane proteins, including TonB-dependent receptors (16). MicF and MicC are also induced by changes in osmolarity and function to repress translation of outer membrane proteins OmpF and OmpC, respectively (12, 17). Though expression of these sRNAs are induced by shifts in the osmotic state of the environment, data demonstrating a role for OmrA/OmrB, MicC, and MicF in cell survival under acute osmotic stress have not been reported to our knowledge.

We have assayed osmotic stress survival of a series of *gsrN* mutant strains, used transcriptomic and proteomic methods to more clearly define the role of GsrN in gene expression during hyperosmotic stress, and provided evidence for a new direct regulatory target of GsrN. Features of GsrN structure that are functionally important for hyperosmotic stress survival are contained in the 5' end of the molecule, and include a conserved cytosine-rich stem loop structure. Transcriptomic and proteomic analyses identified genes that are both activated and repressed by GsrN upon shift to a hyperosmotic environment. Among the regulated gene set was a hypothetical protein we have named OsrP, which contains a glycine zipper domain resembling the glycine zipper motifs of large- and small-conductance mechanosensitive channels (19). We present evidence that GsrN directly interacts with *osrP* mRNA and activates OsrP protein expression at the post-transcriptional level to form a coherent feedforward regulatory loop. This study advances understanding of *Caulobacter crescentus* gene expression during hyperosmotic stress and defines a new post-transcriptional regulatory target of GsrN.

Results

A 5' cytosine-rich loop in GsrN is necessary for osmotic stress survival

GsrN is a small RNA (sRNA) that undergoes endonucleolytic processing, and functions as a potent regulator of both oxidative stress and osmotic stress survival in *Caulobacter crescentus* (11). Expression of the processed 5' fragment of GsrN is necessary and sufficient to protect cells from hydrogen peroxide exposure. This protection requires interaction of GsrN with the mRNA of catalase/peroxidase *katG* through a C-rich loop located in the stable 5' half of GsrN (11). To assess

the functional role of GsrN processing and the 5' C-rich loop under a distinct stress condition, we assayed osmotic stress survival of strains harboring truncated and C-loop mutant variants of GsrN.

For these assays, we generated: *i)* a GsrN deletion strain (Δ*gsrN*), and *ii)* a strain lacking the 5' end of GsrN, *gsrN*(Δ5') (by deleting *gsrN* nucleotides 10-50) (**Fig. 1A**). Both Δ*gsrN* and *gsrN*(Δ5') had ≈1 order of magnitude reduced viability during sucrose-induced osmotic stress when compared to wild-type *Caulobacter* strain CB15 **(Fig. 1B**). Ectopic expression of the first 58 nucleotides of *gsrN* in single copy from its native promoter (*gsrN*(Δ3')) complemented the survival defect of Δ*gsrN*. Notably, a Δ*gsrN* strain harboring multiple integrations of this complementation plasmid, Δ*gsrN*::*gsrN*(Δ3')$^{++}$, had increased viability under hyperosmotic stress compared to wild type (**Fig. 1B**). This protective effect is consistent with peroxide stress protection conferred by full-length *gsrN* overexpression (*gsrN*$^{++}$), reported in our previous study (11).

Given that expression of the 5' end of GsrN complemented the hyperosmotic stress survival defect of Δ*gsrN*, we hypothesized that the 5' C-rich loop functions to mitigate osmotic stress in addition to its previously reported function in peroxide stress mitigation. Overexpression of a GsrN mutant variant in which the 5' cytosine tract was replaced with guanosines, *gsrN*(RS), failed to restore osmotic stress survival to wild-type levels in the Δ*gsrN* strain (**Fig. 1C**). We thus propose that the 5' C-loop of GsrN is necessary to target mRNAs that are involved in osmotic stress survival.

gsrN-dependent osmotic stress protection requires _sigT_

gsrN expression is directly activated by the general stress sigma factor, SigT (σ^T). As described above, strains lacking *sigT* (6, 20) or *gsrN* (11) are susceptible to osmotic stress. We thus tested whether expression of *gsrN* is sufficient to rescue the osmotic stress survival defect of the Δ*sigT* strain, as previously reported for hydrogen peroxide stress (11). We constructed a Δ*sigT* strain in which *gsrN* transcription was driven by the primary sigma factor RpoD (σ^{70}). We call this expression system P1-*gsrN* (**Fig. 2A**). GsrN expressed from P1 had comparable steady-state levels as GsrN expressed from its native σ^T-dependent promoter (**Fig. 2B**), but did not rescue the hyperosmotic stress survival defect of Δ*sigT* (**Fig. 2C**). Unlike acute peroxide stress, osmotic stress induces the transcription of *gsrN* by a

127 factor of three (11). To better emulate GsrN expression during osmotic stress, we further created a
128 strain bearing three copies of P1-*gsrN*. Using this 3(P1-*gsrN*) strain, we matched the enhanced
129 steady-state levels of GsrN observed during osmotic stress (**Fig. 2B**). However, enhanced expression
130 of GsrN in Δ*sigT*+3(P1-*gsrN*) still failed to rescue the hyperosmotic stress survival defect of the Δ*sigT*
131 strain (**Fig. 2C**). We conclude that GsrN-dependent protection during hyperosmotic stress requires σ^T.
132
133 **Defining *sigT* and *gsrN* regulated genes under hyperosmotic conditions**
134 We considered two non-mutally exclusive models to explain why GsrN-dependent protection
135 against hyperosmotic stress requires σ^T: *i)* GsrN functions as a direct post-transcriptional regulator of
136 mRNAs that are transcribed by σ^T, *ii)* GsrN regulates gene products that are not under the control of
137 σ^T, but that require σ^T-regulated genes to mitigate hyperosmotic stress. Thus, to identify candidate
138 mRNA targets and begin gathering evidence to support either or both models, we measured gene
139 expression changes during hyperosmotic stress in a GsrN overexpression strain (*gsrN*$^{++}$), a Δ*sigT*
140 strain, and in wild type *Caulobacter*. Specifically, we measured steady-state transcript levels in Δ*sigT*
141 and wild type strains under stressed and untreated conditions to define the σ^T-dependent osmotic
142 stress regulon. We further measured transcripts in *gsrN*$^{++}$ and wild type under the same conditions to
143 identify candidate transcripts involved in *gsrN*-dependent hyperosmotic stress protection. Lastly, we
144 measured proteome changes between treated and untreated *gsrN*$^{++}$ and wild-type strains to define
145 protein expression regulated by GsrN during osmotic stress.
146 Although *sigT*-dependent gene expression has been previously studied in *Caulobacter* (7, 20,
147 21), a high-resolution expression analysis of GSR mutant strains under hyperosmotic stress has not
148 been published. Our RNA-seq measurements defined a σ^T regulon comprising 333 genes that are
149 differentially expressed between Δ*sigT* and wild type under untreated conditions (false-discovery rate
150 (FDR) *p-value* ≤0 .05; absolute fold change ≥ 1.5). The number of differentially regulated genes during
151 hyperosmotic stress is greater – 530 genes – using the same cutoff criteria. We defined the core σ^T-
152 regulon as the intersection of differentially regulated genes in both untreated and treated conditions,
153 220 genes **(Table S3)**. This greatly expands the number of σ^T-regulated genes compared to previous

reports by our group (20) and others (21). We further sought to predict genes that may be directly transcribed by σ^T based on our gene expression data. To this end, we extracted 250 nucleotide windows upstream of the translation start sites of genes activated by *sigT*. In the case of operons, we only considered the upstream region of the leading gene. Using a degenerate σ^T search motif based on variations observed in 20 identified σ^T-binding sites in past studies **(Fig. S2)** (7, 20, 21), we identified 32 new σ^T-binding sites in the *Caulobacter* genome **(see Table S1)**.

A parallel RNA-Seq experiment identified 35 genes that are differentially expressed in *gsrN*$^{++}$ relative to wild type in untreated conditions and 141 genes under hyperosmotic conditions (false-discovery rate (FDR) *p-value* ≤0 .05; absolute fold change ≥ 2.0) **(see Table S4)**. Considering that differences in GsrN-regulated transcripts do not necessarily correspond to differences in protein levels (11), and that GsrN is known to regulate gene expression at the post-transcriptional level, we further performed a LC-MS/MS analysis of total soluble protein isolated from *gsrN*$^{++}$ and wild type strains under untreated and hyperosmotic conditions. Twenty-two proteins showed significant differences in steady-state levels between *gsrN*$^{++}$ and wild type under untreated conditions (false-discovery rate (FDR) *p-value* ≤0.05; absolute fold change ≥ 2.0). None of these proteins showed significant transcript level differences under the same criteria, though, they all showed significant negative fold change differences in protein abundance **(Table 1)**. This suggests that the predominant role for *gsrN* in exponentially-growing cells might be as a repressor. Protein measurements under hyperosmotic stress revealed nine proteins that had significant differences in steady-state levels between *gsrN*$^{++}$ and wild type **(Table 2)**. Four of these proteins had corresponding significant differences in transcript levels; one protein had an inverse relationship with its transcript levels (**Fig. 3**). This analysis identified proteins whose expression is activated by GsrN and proteins whose expression is repressed by GsrN under hyperosmotic stress.

Comparative RNA-seq analysis uncovers candidate targets of GsrN under hyperosmotic stress

To delineate the roles of *sigT* and *gsrN* in stress survival, we compared genes that are differentially regulated between Δ*sigT, gsrN*$^{++}$ and wild type strains subjected to hyperosmotic stress.

More explicitly, we sought to test the model that GsrN functions as a direct post-transcriptional regulator of mRNAs that are dependent on σ^T-transcription. Since transcription of *gsrN* is directly activated by σ^T, we expected (in this model) that the set of transcripts modulated by *gsrN* overexpression should exhibit some overlap with the set of transcripts that change upon *sigT* deletion. Indeed, we observed 20 genes with congruent patterns of regulation in these two datasets (**Fig. 4A and Table 3**).

Through this comparative approach, we identified six candidate genes that were possibly targeted and upregulated by GsrN. Transcript levels for these genes were significantly lower than wild type in Δ*sigT* and higher in *gsrN*$^{++}$ under hyperosmotic stress (**Fig. 4B**). We predicted strong σ^T-binding sites in the promoters of five of these candidates: *CCNA_00882*, *CCNA_00709*, *CCNA_03889*, and *CCNA_03694-CCNA_03595* (**Table S1**). Of these possible direct regulatory targets of GsrN, *CCNA_00882* showed the highest fold change (≈7 fold) between *gsrN*$^{++}$ and wild type strains subjected to hyperosmotic stress (**Fig. 4B**). Moreover, *CCNA_00882* is strongly upregulated during osmotic stress: in a wild type background, *CCNA_00882* mRNA levels were upregulated ≈6 fold in stressed versus unstressed cultures. In GsrN overexpression strains (*gsrN*$^{++}$), *CCNA_00882* mRNA was further enhanced (≈12.5 fold) in stressed relative to unstressed cultures. Thus, we named *CCNA_00882*, *osrP*, osmotic stress regulated protein. We note that *osrP* mRNA was previously identified as a species that co-elutes with GsrN in an affinity pull-down experiment (11). Considering the presence of a σ^T binding motif in the *osrP* promoter, its regulation by GsrN in our transcriptomic datasets, and the fact that it co-purifies with GsrN, we proposed that o*srP* is a direct target of GsrN.

osrP is regulated by σ^T, induced under hyperosmotic stress, and interacts with GsrN via its 5' leader sequence

osrP is annotated as a 332-residue hypothetical protein that is largely restricted to the genus *Caulobacter*, based on a BLAST search (22) of the GenBank non-redundant database. However, the primary structure of *osrP* shares some features with annotated open reading frames across genera in the family Caulobacteraceae including *Phenylobacterium*, *Asticcacaulis*, and *Brevundimonas*. OsrP

contains a signal peptide at its amino terminus with a Type I signal peptidase cleavage site, as predicted by SignalP (23). A conserved glycine zipper motif (Pfam05433) comprised of two hydrophobic helices is located between residues 224 and 268. Based on these sequence features, we predict that OsrP is a periplasmic protein **(Fig. S3)**.

To better understand the regulation of *osrP* by σ^T and GsrN, we identified its transcription start site (TSS) by 5' rapid amplification of cDNA ends (5' RACE). We mapped the *osrP* TSS to nucleotide 962935 on the *C. crescentus* chromosome; a near-consensus σ^T binding site is positioned at -35 and -10 relative to the *osrP* TSS (**Fig. 5A and Table S1**). To assess transcriptional regulation of *osrP*, we generated a fusion of the *osrP* promoter to a promoterless *lacZ* (**Fig. 5B**). Measured β-galactosidase activities in wild type and Δ*gsrN* strains harboring this reporter plasmid were comparable under untreated conditions, and transcription was activated in both of these genetic backgrounds upon addition of 150 mM sucrose to induce hyperosmotic stress. A Δ*sigT* strain harboring this plasmid had no measureable β-galactosidase activity, and was not induced upon addition of 150 mM sucrose (**Fig. 5B**). We conclude that transcription of *osrP* depends on *sigT* and is independent of *gsrN*.

We previously affinity purified GsrN tagged with a PP7 RNA hairpin aptamer (GsrN(37)-PP7hp) from *Caulobacter* cell lysate, and quantified RNAs that co-purified with GsrN by RNA-seq (11). For this present study, we have re-analyzed our published dataset (NCBI GEO accession number GSE106171) with the goal of identifying reads that map to *osrP* mRNA. We observed significant enrichment of reads that map to the extended 5' leader sequence of *osrP*, which is comprised of approximately 80 nucleotides between the TSS and the annotated start codon. Read density from PP7hp-GsrN(term) (negative PP7 hairpin control) showed no enrichment of the 5' leader of *osrP* (**Fig. 5C**). IntaRNA analysis (24) of this co-purifying region predicted strong base-pairing between the 5' C-rich loop of GsrN and the 5' leader of *osrP* (**Fig. 5A**). From these data, we conclude that GsrN interacts with the 5' untranslated leader of *osrP* mRNA.

GsrN activates OsrP expression at the post-transcriptional level

To test the functional significance of the proposed GsrN binding site in the 5' leader of *osrP* mRNA, we constructed an *osrP* transcriptional-translational (TT) reporter plasmid. The reporter contains the *osrP* promoter, the 5' untranslated region (5' UTR), and the first 7 codons of *osrP* fused to 5' end of *lacZ* lacking a start codon (**Fig. 6A**). The RNA-fold (25) structure of the 5' UTR and the nucleotides encoding the first 7 amino acids of *osrP* predicts that the majority of the GsrN-binding site is sequestered in a base-paired region (26) (**Fig. 6B**). Under unstressed conditions, measured activity from the TT reporter is low in wild type background, but reduced by 2 fold in Δ*sigT* and Δ*gsrN* backgrounds. Overexpression of *gsrN* (*gsrN*$^{++}$) enhances expression by 8 fold compared to wild type. This enhancement of *osrP* expression requires *sigT*, as overexpression of *gsrN* from the σ^{70} P1 promoter in a Δ*sigT* background does not induce expression from the *osrP* TT reporter **(Fig. 6C)**. This result is consistent with data presented in **Fig. 5B** showing the *osrP* transcription requires σ^{T} and supports a model in which GsrN regulates OsrP protein expression at the post-transcriptional level. Lastly, our measurements of *osrP* TT reporter activity under hyperosmotic stress conditions showed similar relative regulatory trends across the assayed genetic backgrounds, though baseline expression is higher (**Fig. 6C**).

To directly validate the OsrP expression reporter data, we inserted a C-terminal FLAG tag at the native *osrP* locus on the *Caulobacter* chromosome. OsrP::M2 is expressed at low levels in exponentially growing wild type cultures, and was difficult to detect by Western blot. However, we observed increased steady-state levels of OsrP::M2 in exponential phase cultures of the *gsrN*$^{++}$ strain (**Fig. 6D**). To assess the effects of hyperosmotic stress of *gsrN* on OsrP expression, we added 150 mM sucrose to cultures of wild type, Δ*gsrN*, and *gsrN*$^{++}$. Hyperosmotic stress induced the production of OsrP::M2 in wild type and this effect largely required *gsrN*; there was no detectable OsrP::M2 signal in Δ*gsrN*. Consistent with our *osrP* reporter data, we observed a large increase in OsrP::M2 levels in *gsrN*$^{++}$ relative to wild type during hyperosmotic stress (**Fig. 6D**). Again, these data support a model in which GsrN activates OsrP protein expression at the post-transcriptional level.

Assessing the role of the GsrN C-rich recognition loop in activation of OsrP expression

It is established that the C-rich target recognition loop is a functionally-important feature of GsrN structure that directly activates KatG catalase/peroxidase expression through a base-paring interaction with the 5' leader of *katG* mRNA (11). To test the role of the GsrN recognition loop in the activation of OsrP protein expression, we constructed a TT *osrP* reporter containing RS mutations in the 5' leader of *osrP* (*osrP*-RS1), which are predicted to restore G-C base pairing with the GsrN(RS) recognition loop mutant (see **Fig. S4**).

The *osrP*-RS1 reporter showed no difference in activity between wild type and Δ*gsrN* in untreated conditions, though basal expression from this reporter was higher than the wild-type *osrP* TT reporter. Expression from the *osrP*-RS1 reporter was equivalently induced in hyperosmotic conditions in wild type and Δ*gsrN* backgrounds; *osrP*-RS1 reporter activity was modestly induced (2-fold) in *gsrN*$^{++}$ relative to wild type **(Fig. S4B)**. However, the magnitude of induction was considerably diminished relative to the 8-fold induction we observed from the wild-type *osrP* TT reporter upon *gsrN* overexpression **(Fig. 6C)**. We did not observe significant differences in *osrP*-RS1 reporter activity under hyperosmotic stress in wild type, Δ*gsrN,* and *gsrN*++ strains. We further introduced the *osrP*-RS1 reporter into the *gsrN*(RS) mutant strain. Again, we observed elevated expression from the *osrP*-RS1 reporter relative to the wild type *osrP* TT reporter in both wild type and *gsrN*(RS) backgrounds (**Fig. S4C**). These experiments therefore failed to uncover direct evidence for base pairing interaction between the GsrN recognition loop and the predicted target site in the 5' leader of *osrP*.

However, we noted that the 5' leader mutations in *osrP*-RS1 would disrupt the predicted secondary structure of the *osrP* leader **(see Fig. S4A)**, which may influence GsrN-dependent regulation. To compensate for base pairing disruptions introduced in *osrP*-RS1, we generated compensatory base changes on the opposing arm of the RNA stem that would be predicted to restore leader secondary structure; we termed this the *osrP*-RS2 reporter **(Fig. S4D)**. We failed to detect any reporter activity from *osrP*-RS2 in any strain, including strains expressing *gsrN(RS)* (**see Fig. S4E-F**). Based on these reporter data, we conclude that mutation of the predicted GsrN target site in the 5' leader of *osrP* derepresses expression of OsrP protein. From this set of experiments, we are not able

to definitively conclude that there is a base pairing regulatory interaction between the GsrN C-rich recognition loop and the 5' leader of *osrP* mRNA that activates OsrP expression.

osrP is not major genetic determinant of hyperosmotic stress survival

Given that *osrP* expression is under strong positive control of σ^T and GsrN during hyperosmotic stress, we tested the possibility that *osrP* contributes to stress survival. Deletion of *osrP* (Δ*osrP*) did not affect the viability of *C. crescentus* under hyperosmotic conditions when compared to wild type and Δ*gsrN* strains **(Fig. S1D)**. We also expressed *osrP* from a xylose-inducible expression plasmid that we integrated into the chromosomal *xylX* locus, (*osrP*$^{++}$). Similar to Δ*osrP*, the viability of the *osrP*$^{++}$ strain in the presence of inducer did not did not differ significantly from wild type **(Fig. S1D)**. We further tested the effects of deletion and overexpression of *osrP* on osmotic stress survival in Δ*gsrN* and *gsrN*$^{++}$ backgrounds. Δ*gsrN osrP*$^{++}$ viability did not differ significantly from Δ*gsrN* and Δ*osrP gsrN*$^{++}$ did not differ significantly from *gsrN*$^{++}$ **(Fig. S1D)**. From these data, we conclude that *osrP* is not a major contributor to hyperosmotic stress survival under the assayed conditions.

Discussion

Microbes employ regulatory systems that function to mitigate the effects of osmotic stress (27). During hyperosmotic stress, the freshwater oligotroph *Caulobacter crescentus* activates the general stress response (GSR) sigma factor, σ^T, which in turn activates transcription of a large set of genes **(Table S3)** including the sRNA, GsrN (11, 21). Deleting either *sigT* or *gsrN* results in reduced viability under sucrose-induced hyperosmotic stress **(Fig.1C and Fig. 2C)**. *gsrN*-dependent cell protection during hyperosmotic stress requires *sigT* **(Fig. 2C)**.

Transcriptomic analysis of a Δ*sigT* strain provided a comprehensive view of the σ^T hyperosmotic stress regulon, while transcriptomic and proteomic analysis of a *gsrN* overexpression strain (*gsrN*$^{++}$) revealed a set of transcripts and proteins that are under post-transcriptional control of GsrN during hyperosmotic stress **(Fig. 3 and Table 2)**. Comparative analyses of these datasets provided evidence for multi-output feedforward loops (FFL) involving σ^T and GsrN. One such coherent

FFL involves the uncharacterized glycine-zipper protein, OsrP. Specifically, transcription of *osrP* is activated by σ^T **(Fig. 5B)**, likely via the canonical σ^T binding site in its promoter **(Fig. 5A and Table S3)**. OsrP protein expression is activated at the post-transcriptional level by GsrN **(Fig. 6C-D)**, to form a coherent FFL. Both *sigT* and *gsrN* are required for OsrP protein expression; thus, both regulators comprise an AND gate that regulates *osrP*.

A coherent feedforward loop controls a *Caulobacter* gene expression response during hyperosmotic stress

Feedforward loops (FFL) are common regulatory motifs in microbial gene expression networks. In their simplest form, FFLs are comprised of three genetic components: two regulators and an output gene. The primary regulator functions to activate both the secondary regulator and the output gene; the secondary regulator functions to activate expression of the output gene (28). In the case of *osrP*, σ^T is the primary regulator that activates *osrP* and *gsrN* transcription; GsrN interacts with *osrP* mRNA to activate OsrP protein expression at the post-transcriptional level **(Fig. 7)**.

There are several examples of sRNAs that are part of FFL motifs in bacteria (29-31). Activation of *osrP* expression by σ^T and GsrN is perhaps most similar to the regulation of *ricI*, an inhibitor of conjugation in *Salmonella*, by σ^S and the sRNA RprA (30). In this instance, the primary and secondary regulators are swapped: RprA acts as a primary activator of *rpoS* and *ricI* expression. RprA itself is activated by the Rcs system (32), which responds to envelope stress. However, *rpoS* expression is determined by multiple environmental signals and does not require *rprA* to transcribe *ricI*. Thus, *ricI* can be transcribed in the absence of envelope stress, but both RprA and σ^S are required for RicI protein expression. Thus, RprA and σ^S function as a FFL AND gate that ensures RicI expression only occurs upon Rcs activation by envelope damage.

Unlike *ricI*, the coherent FFL controlling *osrP* is activated by σ^T alone. In wild-type *C. crescentus*, we observe basal σ^T-dependent gene expression in the absence of any apparent stress **(Fig. 5B and Fig 6C)**. During hyperosmotic stress, *osrP* expression measured from the *osrP i)*

transcription and *ii)* transcription plus translation (TT) reporters are incongruent: *osrP* transcription increases 2-fold during hyperosmotic stress while TT reporter activity increases 6-fold within an equivalent time window. The difference in fold change between the two reporters is likely due to the positive regulatory effects of GsrN. The increased fold change of the TT reporter can be attributed to the 3-fold increase of GsrN during hyperosmotic stress (11). In fact, *osrP* TT-reporter activity increased 6-7 fold upon *gsrN* overexpression in both stressed and unstressed conditions.

During persistent stress conditions, such as hyperosmotic stress and stationary phase, we have observed that the more stable 5' isoform of GsrN accumulates to higher levels than full-length GsrN (11). Accumulation of the 5' GsrN isoform could act as signal within the *sigT*-regulon to mount a specific response to persistent stress, such as hyperosmotic shock. This model is consistent with AND-type coherent FFLs, which result in delayed activation of the output gene. Expression delay arises from the lag between the production of the secondary regulator and the threshold necessary for the secondary regulator to act upon the output gene (28). In the case of *osrP*, levels of GsrN may set the threshold for OsrP protein production. Accumulation of the 5' GsrN isoform through prolonged σ^T-activity could amplify the expression of *osrP* over other σ^T-regulated genes in particular stress regimes. Although we conclusively demonstrate only one GSR coherent feedforward loop (during hyperosmotic stress) in this study, our transcriptomic and proteomic data show that several genes in the GSR regulon may be subject to similar regulation.

Functional analysis of the uncharacterized glycine zipper protein, OsrP

Bioinformatic analysis of OsrP predicts two notable features in its sequence: a signal peptide at its amino terminus with a Type I signal peptidase cleavage site and a conserved glycine zipper motif (Pfam05433) **(Fig. S3)**. From this analysis, we predict that OsrP is in the periplasm of *C. crescentus*. The primary structure of the glycine zipper motif suggests a possible interaction with the cell membrane. Extended glycine zipper motifs can oligomerize and form pores within membranes (19). One notable example is the secreted VacA toxin of *H. pylori* that forms a hexameric anion selective channel in host cells (33).

In considering its primary structure, predicted localization, and regulation, it seemed possible that *osrP* could help alleviate osmotic stress in *C. crescentus.* However, deletion of *osrP* did not result in any obvious viability defect during sucrose-induced hyperosmotic stress. Considering there are several genes co-regulated by σ^T and GsrN, it may be the case that additional genes are required to mitigate the hyperosmotic stress conditions that we have tested. Prolonged exposure to other osmotic stresses and/or different concentrations of osmolytes – including a range of ions – could provide insight into function of *osrP* activation by the GSR.

In a recent study of a diverse set of bacterial species, including *C. crescentus*, growth of transposon mutant libraries was characterized under multiple environmental conditions (34). In *C. crescentus*, *osrP* disruption resulted in a consistent disadvantage in growth in the presence of sodium perchlorate (fitness = -1.3, t score =-7.2). Sodium perchlorate is an anionic oxidizing agent. It remains uncertain how the oxidative, osmotic (or other) effects of sodium perchlorate in the medium affect fitness of strains harboring transposon disruptions of *osrP*, but this result provides an additional assay condition for future functional studies of *osrP*.

On additional GsrN regulatory targets

Proteomic analysis of the *gsrN*$^{++}$ strain showed strikingly different sets of regulated genes between untreated and hyperosmotic stress conditions. In untreated cultures of *gsrN*$^{++}$, all proteins with significant differential expression were under negative control of GsrN; there was no overlap with the differentially expressed proteins we observed in stress-treated cultures. Although GsrN may not directly control expression of all differentially regulated proteins in this dataset, the effect we observe upon *gsrN* overexpression in the absence of stress points to a role for GsrN during normal growth **(Table 1)**. Notably, the cell-cycle phosphotransfer protein ChpT is significantly downregulated in the *gsrN*$^{++}$ strain. ChpT is an essential protein is required for phosphorylation of the essential cell-cycle master regulator, CtrA (35). Given the established connection between levels of CtrA and σ^T during nutrient limitation (36), it is conceivable that GsrN regulates the core cell cycle control system of *C. crescentus* under certain conditions.

Under hyperosmotic conditions, we observed only a few cases of proteins that differ in steady-state levels between *gsrN*$^{++}$ and wild type. Among the negatively regulated proteins are three TonB-dependent receptors of unknown function (*CCNA_00028*, *CCNA_00214*, and *CCNA_3023*) and a predicted efflux complex (*CCNA_02172-74*) **(Tables 2 and 3)**. GsrN may therefore have a functional role that is similar to the sRNAs, MicA and RybB, which are transcribed during envelope stress by σ^E in *E. coli* and repress outer membrane proteins (OMP) to mitigate accumulation of unfolded OMPs (37).

Among the genes activated at the transcript level by GsrN during hyperosmotic stress are several with predicted σ^T-binding sites in their promoters (*CCNA_00709*, *CCNA_03889*, and *CCNA_03694-CCNA_03595*), which may provide additional cases of coherent FFLs. As discussed previously, expression of these genes may be sensitive to GsrN accumulation during prolonged stress. CCNA_00709 – a predicted small, two-pass membrane protein – and CCNA_03694 – a transcription factor – are attractive targets to investigate in future studies on the mechanism by which GsrN determines cell survival during hyperosmotic stress.

Materials and Methods

All *C. crescentus* experiments were conducted using strain CB15 (38) and derivatives thereof.

Growth of *E. coli* and *C. crescentus*. *C. crescentus* was cultivated on peptone-yeast extract (PYE)-agar (0.2% peptone, 0.1% yeast extract, 1.5% agar, 1 mM $MgSO_4$, 0.5 mM $CaCl_2$) (39) supplemented with 1.5% agar at 30°C. Antibiotics were used at the following concentrations on this solid medium: kanamycin 25 mg/ml, tetracycline 2mg/ml, nalidixic acid 20 mg/ml, and chloramphenicol 2 mg/ml. For liquid culture, *C. crescentus* was cultivated in either PYE or in M2X defined medium (39). PYE liquid: 0.2%(w/v) peptone, 0.1%(w/v) yeast extract, 1 mM $MgSO_4$, and 0.5 mM $CaCl_2$, autoclaved before use. M2X defined medium: 0.15% (w/v) xylose, 0.5 mM $CaCl_2$, 0.5 mM $MgSO_4$, 0.01 mM Fe Chelate, and 1x M2 salts, filtered with a 0.22 micron bottle top filter. One liter of 20x M2 stock was prepared by mixing 17.4 g Na_2HPO_4, 10.6 KH_2PO_4, and 10 g NH_4Cl. Antibiotics were used at the following

concentrations in liquid medium: kanamycin 5 mg/ml, tetracycline 1 mg/ml, and chloramphenicol 2 mg/ml. For cultivation of *E. coli* in liquid medium, we used lysogeny broth (LB). Antibiotics were used at the following concentrations: kanamycin 50 mg/ml, tetracycline 12 mg/ml, and chloramphenicol 20 mg/ml.

Plasmid transformation into *C. crescentus*. Plasmids were conjugated into CB15 (39) using the *E. coli* helper strain FC3 (40)**(see Table S1)**. Conjugations were performed by mixing the donor *E. coli* strain, FC3, and the CB15 recipient strain in a 1:1:5 ratio. Mixed cells were pelleted for 2 min at 15,000xg, resuspended in 100 mL, and spotted on a nonselective PYE-agar plate for 12–24 hr. Exconjugants containing the desired plasmid were selected on PYE agar containing the plasmid-specified antibiotic for selection and antibiotic nalidixic acid (20 mg/ml) to counter-select against both *E. coli* strains (helper and plasmid donor). Plasmids pMT552 and pMT680 integrate into the *vanA* and *xylX* locus respectively. pMT680 carries a chloramphenicol resistance marker gene (*cat*) and pMT552 carries a kanamycin resistance marker gene (*npt1*) (41). pNPTS138 integration occurs at a chromosomal site homologous to the insertion sequence.

Chromosomal deletion and allele replacement in *C. crescentus*. To generate the in-frame deletion and C-terminal FLAG-tagged *osrP* (*CCNA_00882*) alleles (Δ*osrP* and *osrP::M2*, respectively), we implemented a double crossover recombination strategy using the pNPTS138 plasmid (42, 43). Briefly, an in-frame deletion allele of *osrP* was generated using primers listed in **Table S2** in the supplemental material and combined using splice-overlap-extension. The deletion allele carries a 5' (UP) and 3' (DOWN) flanking sequences of *osrP* and was ligated in the multiple cloning site (MCS) of a digested pNPTS138 using the restriction enzymes HindIII and SpeI. The tagged allele *osrP::M2* was generated using three pieces, two with primers and one with a gene block (Gblock) listed in **Table S2**. The tagged allele was inserted using Gibson assembly of all three pieces and the same cut plasmid of the Δ*osrP* plasmid. The first recombination was achieved using a tri-parental mating described in the "Plasmid integration in *C. crescentus*" section with the plasmid-specified antibiotic,

kanamycin (5 mg/ml). Single colony exconjugants were inoculated into liquid PYE for 6–16 hours in a rolling 30°C incubator for non-selective growth. Nonselective liquid growth allows for the second recombination event to occur, which either restores the native locus or replaces the native locus with the pNPTS138 insertion sequence. Counter-selection for the second recombination of pNPTS138 was carried out on PYE agar with 3% (w/v) sucrose. This selects for loss of the *sacB* gene during the second recombination event. Colonies were subjected to PCR genotyping and/or sequencing to confirm the allele replacement.

Complementation construction in *C. crescentus*. Tandem P1-*gsrN* alleles (overexpression by multiple copies of P1-*gsrN*) were constructed using a Gblock template amplified with three sets of unique primers. Each end of the amplified products contained unique overlap ends for Gibson assembly into pMT552 digested with KpnI and SacI. *gsrN* alleles cloned into the *vanA* locus are antisense to the vanillate inducible *vanA* promoter. An in-frame stop codon was designed at the restriction enzyme/ligation site downstream of the *vanA* promoter to ensure that translational read-through of the *vanA* transcript did not disrupt *gsrN* transcription. Xylose-inducible *osrP* (pMT680-*osrP*) had its entire coding sequence cloned in frame with the start site of *xylX*.

β-galactosidase reporter construction in *C. crescentus*. Transcriptional and transcriptional-translational (TT) reporters utilized the replicating plasmids pRKlac290 and pPR9TT, respectively (39, 44). pRKlac290 has a tetracyline resistance marker and pPR9TT has a chloramphenicol resistance marker. Insertion sequences of *osrP* used the primers in **Table S2**. The template for *osrP(RS1)* was created using splice-overlap-extension and the template for *osrP(RS2)* was a gblock. Templates were then amplified with the same primers as the wild-type *osrP* reporters. The transcriptional reporter used the restriction sites EcoRI and HindIII to ligate into pRKlac290. The transcriptional-translational reporter used the restriction sites KpnI and HindIII to ligate into pPR9TT.

475 **Osmotic stress assay.** Liquid cultures were passaged several times before stress treatment to
476 insure that population growth rate and density were as consistent as possible prior to addition of
477 sucrose (hyperosmotic stress). Briefly, starter cultures were inoculated in liquid M2X medium from
478 colonies grown on PYE-agar plates. Cultures were grown overnight at 30°C in a rolling incubator.
479 Overnight cultures were then diluted back to an optical density reading of OD_{660} = 0.05 and grown in a
480 rolling incubator at 30°C for 7–10 hr. After this period, cultures were re-diluted with M2X to OD_{660} =
481 0.025 and grown overnight for 16 hr at 30°C in a rolling incubator. After this period, OD_{660} was
482 consistently 0.85–0.90. These cultures were then diluted to OD_{660} = 0.05 and grown for 1 hr and split
483 into two tubes. One tube received sucrose treatment from a liquid stock of 80% (w/v) and the other
484 tube was treated with water. Both cultures were grown for 5 hours in a rolling 30°C post treatment of a
485 final concentration of 300 mM sucrose. This allowed for the dynamic range to compare CFUs from
486 Δ*gsrN*, wild type, and *gsrN*$^{++}$. Treated cultures and untreated cultures were subsequently titered (10
487 mL sample in 90 mL of PYE) by initially diluting into 96-well plates. 5 mL spots from each dilution were
488 plated on PYE-agar. Once spots dried, plates were incubated at 30°C for 2 days. Clearly visible
489 colonies begin to form after 36 hours in the incubator.
490
491 **Northern Blot.** RNA samples were resolved on a urea-denaturing 10% acrylamide: bisacrylamide
492 (29:1), tranferred onto a Zeta-Probe Blotting Membrane with a Trans-Blot® SD Semi-Dry Transfer Cell.
493 Blots were hybridized with a hybridization buffer containing the radiolabeled oligonucleotide probes in
494 a rolling 65°C incubator. Hybridization buffer had a GsrN probe concentration ~1 nM and 5S rRNA
495 probe concentration was ~2 pM. Membranes were then wrapped in plastic wrap and placed directly
496 against a Molecular Dynamics Phosphor Screen. Screens were imaged with Personal Molecular
497 Imager™ (PMI™) System. For detailed buffer recipes and step-by-step instructions refer to (11).
498 Cultures used for the extraction of RNA were passaged in the same manner outlined in the “Osmotic
499 stress assays” section above. Exponential phase cultures were harvested from the last starter (i.e.,
500 the OD_{660}=0.05 culture at the 16 hour time point) when it reached an OD_{660} of 0.20-0.25. Exponential
501 phase cultures (OD_{660} of 0.20-0.25) harvested for extraction of RNA were pelleted at 15000x g for 3

minutes at ≈23°C (i.e. room temperature) and subjected to a TRIzol extraction (refer to detailed protocol (11)). Radiolabeled oligonucleotides were labeled with T4 PNK (refer to (11) for detailed protocol). Oligonucleotide sequences used for Northern blot probing can be found in **Table S2** in the supplement material.

RNA-Seq sample preparation and analysis. RNA-Seq samples were extracted using the TRIzol protocol described in (11). For the first RNA-Seq experiment with seven Δ*sigT* (3 stressed and 4 unstressed) and eight WT (4 stressed and 4 unstressed) samples, cells were grown similarly to those described in the "Osmotic stress assay" section. Specifically, liquid M2X cultures were inoculated from PYE agar plates and grown shaking at 200 RPM, 30°C overnight. Cultures were then diluted into fresh M2X to OD_{660} = 0.025 and grown at 200 RPM, 30°C for 18 hours. These overnight cultures were then diluted to OD_{660} = 0.15, and grown for 1 hour at 200 RPM, 30°C before the addition of 150 mM Sucrose (treated) or water (untreated). Samples were grown for 3 hours at 200 RPM, 30°C before TRIzol extractions. Resuspended RNA pellets after the 75% ethanol wash were purified twice by RNeasy Mini Kit column (100 µL sample, 350 µL RLT, 250 µL 100% ethanol). In each iteration, immobilized RNA was subjected to an on-column DNase digestion with TURBO™ DNase for 30 minutes at 30°C with 70 µL DNase Turbo (7 µL DNase, 7µL 10X Buffer, 56µL diH_2O) before washing and elution. For the second RNA-Seq experiment with 8 *gsrN*$^{++}$ (4 stressed and 4 unstressed) and 6 WT (3 stressed and 3 unstressed) samples, cells were grown as described in the "Osmotic stress assay" section. Specifically, treated cultures were grown for 5 hours in M2X with a final concentration 150 mM sucrose and untreated with water in a rolling 30°C incubator before TRIzol extractions. Resuspended RNA pellets after the 75% ethanol wash were loaded onto an RNeasy Mini Kit column (100 µL sample, 350 µL RLT, 250 µL 100% ethanol). Immobilized RNA was then subjected to an on-column DNase digestion with TURBO™ DNase. DNase treatment was repeated twice on the same column; each incubation was 30 minutes at 30°C with 70 µL solutions of DNase Turbo (7 µL DNase, 7 µL 10x Buffer, 56 µL diH2O). For all RNA-seq samples, after elution from the RNeasy column, rRNA was depleted using Ribo-Zero rRNA Removal (Gram-negative bacteria) Kit (Epicentre). RNA-seq

libraries were prepared with an Illumina TruSeq stranded RNA kit according to manufacturer's instructions. The libraries were sequenced on an Illumina HiSeq 4000 at the University of Chicago Functional Genomics Facility. Analysis of whole genome RNA-seq data was conducted using the CLC Genomics Workbench version 11.0. Reads were mapped to the *C. crescentus* NA1000 genome (accession CP001340.1) (45).

Soluble protein extraction for LC-MS/MS and analysis. Total soluble protein for proteomic measurements was extracted from cultures passaged similarly to the “Osmotic stress assays” section, except that cultures were subjected to 150 mM sucrose. Cells were spun down at 8000g at 4°C for 15 minutes. Cells were resuspended in 6 mL of ice-cold lysis buffer. Cells were mechanically lysed in LV1 Microfluidizer. Lysate was then spun down at 8000g at 4°C for 15 minutes. Protein samples were resolved on a 12% MOPS buffered 1D Gel (Thermo Scientific) for 10 minutes at 200V constant. Gel was stained with Imperial Protein stain (Thermo Scientific), and a ~2 cm plug was digested with trypsin. Detailed trypsin digestion and peptide extraction by the facility is published in (46). Samples for analysis were run on an electrospray tandem mass spectrometer (Thermo Q-Exactive Orbitrap), using a 70,000 RP survey scan in profile mode, m/z 360-2000 Fa, with lockmasses, followed by 20 MS/MS HCD fragmentation scans at 17,500 resolution on doubly and triply charged precursors. Single charged ions were excluded, and ions selected for MS/MS were placed on an exclusion list for 60s (46). Raw files of LC-MS/MS data were processed using the MaxQuant software suite v1.5.1.2 (47). Samples were run against a FASTA file of proteins from the UniProt database (UP000001364) and standard contaminants. The label free quantitation (LFQ) option was turned on. Fixed modification included carbamidomethyl (C) and variable modifications were acetyl or formyl (N-term) and oxidation (M). Protein group files were created for two comparisons: wild-type (3 samples) versus *gsrN*$^{++}$(4 samples) untreated and wild-type (3 samples) versus *gsrN*$^{++}$ (4 samples) sucrose-treated. LFQ values for each proteingroup.txt file were extracted for analysis. Average LFQ values were only calculated if 2 or more LFQ values were found for wild-type samples and if 3 or more LFQ values were found for *gsrN*$^{++}$ samples. This allowed for protein groups that had a sufficient amount of signal

556 across all the samples and analyses to be considered for comparison. Once averages for each
557 protein group were calculated, we calculated the fold change between samples from different
558 backgrounds by dividing the averages and taking the log-2 transformation, log_2(Fold). Multiple t-tests
559 were conducted using the LFQ criteria described previously. We used the multiple t-test analysis from
560 GraphPad Prism version 7.0 for MacOS, GraphPad Software, La Jolla California USA,
561 www.graphpad.com. The false discovery rate (Q) value was set to 5.000% and each row was
562 analyzed individually, without assuming a consistent SD.
563
564 **σ^T-binding site search.** A binding site search was conducted on negative differentially regulated
565 genes identified in the RNA-Seq study (i.e. genes downregulated in Δ*sigT* relative to wild type; fold
566 change ≤ -1.5 and FDR ≤ 0.05) (**Table S3**). From this set of genes, we organized all genes into
567 operon units based on the DOOR database (48, 49); however, we only put a gene into the context of
568 an operon if the leading gene in the operon was also in the core *sigT* regulon. We then took the lead
569 genes for each operon and searched 250 nucleotides upstream of the annotated coding start site.
570 These windows were then scanned for the degenerate σ^T-binding site combinations described in **Fig.**
571 **S2**.
572
573 **5' rapid amplification of cDNA ends (RACE).** Rapid amplification of cDNA 5'ends of GsrN was
574 carried out using components of the FirstChoice RLM-RACE Kit. Cloning of cDNA library was carried
575 out with the Zero Blunt TOPO PCR Cloning Kit. Total RNA from *gsrN*$^{++}$ strains was extracted from
576 stationary phase cultures (OD660 = 0.95–1.0) as described in the "Northern Blot" section. Briefly, 10
577 mL Tobacco Acid Pyrophosphatase (TAP) reactions used 5 mg of total RNA with 2 mL of TAP and 1
578 mL of TAP buffer with remaining volume comprised of Nuclease-free water. Reactions were incubated
579 at 37°C for 1 hour. TAP-treated samples were then subjected to ligation in parallel with no-TAP total
580 RNA samples. Tap RNA sample ligation reactions (10 mL) follow: 2 mL of TAP treated RNA, 1 mL of
581 5'RACE adaptor, 1 mL of T4 RNA Ligase, 1 mL 10X T4 RNA Ligase Buffer, and 4 mL Nuclease-free
582 water. No-TAP RNA sample ligation reactions (10 mL) follow: 3 mg of untreated total RNA, 1 mL of

583 5'RACE adaptor, 1 mL of T4 RNA Ligase, 1 mL 10X T4 RNA Ligase Buffer, and remaining volume of
584 Nuclease-free water. Reactions were incubated at 37°C for 1 hr. For the reverse transcription reaction
585 (first strand synthesis), we used the random dodecamer provided in the kit, as well as, the M-MLV
586 Reverse transcriptase and used the recommended reaction volumes in the kit. Reaction was
587 incubated at 42°C for 1 hour. Samples were then kept frozen in a -20°C freezer. For second strand
588 synthesis and amplification, we used KOD Hot Start DNA Polymerase with the 5'RACE inner primer
589 complementary to the adapter and an *osrP*-specific primer 380 nucleotides away from the coding start
590 site **(Table S2)**. The 25 mL reactions follow: 12.5 mL 2X Buffer, 0.5 mL KOD Polymerase, 5 mL of 2
591 mM dNTP, 2.5 mL of 50% DMSO, 1.5 mL of 5 mM forward primer, 1.5 mL of 5 mM reverse primer,
592 and 1.5 mL of reverse transcribed 1st strand synthesis cDNA. Reaction protocol follows: 3 min 95°C
593 incubation, followed by a 35-cycle reaction consisting of a 15 s 95°C melting step, a 15 s 60°C
594 annealing step, a 30 s 68°C extension step, and a final 1 min 68°C extension step. PCR products
595 were blunt-cloned using the Zero Blunt TOPO PCR Cloning Kit. First, a 5 mL pre-reaction mix
596 consisting of 2 mL PCR product, 1 mL kit salt solution, and 2 mL water was prepared. 1mL of the
597 pCR-Blunt II-TOPO was then added to the pre-reaction mix and incubated at room temperature for 5
598 min and then immediately put on ice. Ligation reaction was then incubated with ice-thawed chemically
599 competent *E. coli* cells for 5 min. Cells were heat shocked for 30 s at 42°C, then incubated on ice for 5
600 min. 250 mL of SOC media was then added to the cells and incubated 37°C in a shaking incubator.
601 Fifty microliters of outgrown cells were placed on LB-Kanamycin plates with an antibiotic
602 concentration of 50 mg/mL. Single colonies were grown overnight and sequenced with an internal
603 *osrP* specific primer that maps 300 nucleotides from the annotated coding start and M13R primers
604 **(Table S2)**. Sequences were submitted to the University of Chicago Comprehensive Cancer Center
605 DNA Sequencing and Genotyping Facility. Chromatograph traces were analyzed with Geneious
606 11.0.2. Traces were subjected to mapping and trimming of the 5'RACE inner primer/adaptor
607 sequence and the flanking regions used for blunt-cloning.
608

609 **β -galactosidase assay.** To assess reporter gene expression, liquid cultures were passaged several
610 times as described in the "Osmotic stress assay" section above. However, cultures were placed in a
611 30°C shaker instead of a 30°C rolling incubator. Exponential phase cultures were taken from the
612 OD_{660} = 0.05 culture made from the 16 hr overnight culture and split when an OD_{660} ~.09-0.1 was
613 reached. One split culture was treated to a final concentration of 150 mM sucrose and the other with
614 the equal volume of water. Stress and unstressed cultures were then grown for three hours in a 30°C
615 shaker and then harvested. β-galactosidase activity from chloroform-permeabilized cells was
616 measured using the colorimetric substrate o-nitrophenyl-b-D-galactopyranoside (ONPG). 1 mL
617 enzymatic reactions contained 350 mL of chloroform-permeabilized cells, 550 mL of Z-buffer (60 mM
618 Na_2HPO_4, 40 mM, NaH_2PO_4, 10 mM KCl, 1 mM $MgSO_4$), and 200 mL of 4 mg/mL ONPG in 0.1 M
619 KPO_4, pH 7.0. Chloroform-permeabilized cell samples were prepared from 150 mL of culture, 100 mL
620 of PYE, and 100 mL of chloroform (chloroform volume is not included in the final calculation of the 1
621 mL reaction). Chloroform-treated cells were vortexed for 5–10 seconds to facilitate permeabilization. Z
622 buffer and ONPG were added directly to chloroform-permeabilized cells. Reactions were incubated in
623 the dark at room temperature and quenched with 1 mL of 1 M Na_2CO_3. Each reporter construct was
624 optimized with different reaction times empirically determined by the development of the yellow ONPG
625 pigment. Miller units were calculated as:

$$MU = \frac{A_{420} \times 1000}{A_{660} \times t \times v}$$

626 A_{420} is the absorbance of the quenched reaction measured at 420 nm on a Spectronic Genesys 20
627 spectrophotometer (ThermoFisher Scientific, Waltham, MA). A_{660} is the optical density of the culture of
628 cells used for the assay. *t* is time in minutes between the addition of ONPG and the quenching with
629 Na_2CO_3. *v* is the volume in milliliters of the culture added to the reaction.
630
631 **Western Blot.** Strains from which protein samples were prepared for Western blot analysis were
632 grown and passaged as outlined in the "Osmotic stress assays" section; however, cultures were
633 grown to an OD_{660}=0.25-0.30, split, and treated with 150 mM sucrose for 3.5 hours. This change

allowed for detection of *osrP::M2* signal in untreated *gsrN*$^{++}$ cultures and treated wild-type cultures. 4.5 mL of these cultures was then pelleted, resuspended in 100 µL of Western blot buffer (10 mM Tris pH 7.4, 1 mM $CaCl_2$, and 5 µg/mL of DNase), and mixed with 100 µL SDS-Loading buffer. Samples were boiled at 85°C for 10 minutes, and 25-30 µL of each sample was loaded onto a Mini-PROTEAN TGX Precast Gradient Gel (4-20%) with Precision Plus Protein™ Kaleidoscope™ Prestained Protein Standards. Samples were resolved at 35 mA constant current in SDS running buffer (0.3% Tris, 18.8% Glycine, 0.1% SDS). Gels were run until the 25 kDa marker reached the bottom of the gel. Gel was transferred to an Immobilon®-P PVDF Membrane using a Mini Trans-Blot® Cell after preincubation in Western transfer buffer (0.3% Tris, 18.8% Glycine, 20% methanol). Transfer was carried out at 4°C, 100 V for 1 hour and 20 minutes in Western transfer buffer. The membrane cut into two pieces right above the 50kD marker. Top half was stained with Coommassie Brilliant Blue for 10 minutes, washed with 45% Ethanol and 10 % Acetic acid, and then washed again with 90% Ethanol 10% Acetic acid. Upon destaining, image was taken with a ChemiDoc MP Imaging System version 6.0. Bottom half was blocked in 5% (w/v) powdered milk in Tris-buffered Saline Tween (TBST: 137 mM NaCl, 2.3 mM KCl, 20 mM Tris pH 7.4, 0.1% (v/v) of Tween 20) overnight at room temperature on a rotating platform. Primary incubation with a DYKDDDDK(i.e. M2)-Tag Monoclonal Antibody (clone FG4R) was carried out for 3 hours in 5% powdered milk TBST at room temperature on a rotating platform (4 µL antibody in 12 mL). Membrane was then washed 3 times in TBST for 5 minutes each at room temperature on a rotating platform. Secondary incubation with Goat anti-Mouse IgG (H+L) Secondary Antibody, HRP was for 1 hour at room temperature on a rotating platform (3 µL antibody in 15 mL). Finally, membrane was washed 3 times in TBST for 10 minutes each at room temperature on a rotating platform. Chemiluminescence was performed using the SuperSignal™ West Femto Maximum Sensitivity Substrate and was imaged using a ChemiDoc MP Imaging System version 6.0. Chemiluminescence was measured using the ChemSens program with an exposure time of ~2.5 minutes.

660 **Accession number(s).** RNA-Seq data are available in the NCBI GEO Database under accession
661 GSE114971. LC-MS/MS data is available in the PRIDE proteomic database under accession
662 PXD010072.

663

664 **Acknowledgements**

665 This work was funded by NIH award R01GM087353 to SC. M.Z.T was supported by an NSF
666 Graduate Research Fellowship, and B.J.S. is supported by NIH award F32GM128283.

667

668

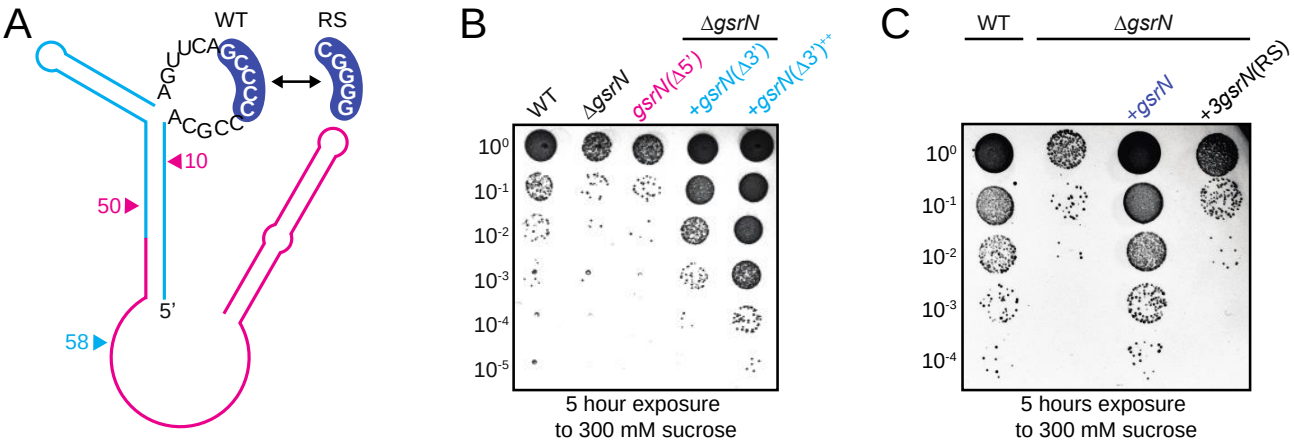

FIG 1 Modifying the 5' cytosine-rich loop of GsrN reduces *Caulobacter* viability under hyperosmotic stress. (A) Secondary structure model of GsrN. Bases in the 5' C-rich loop are displayed. GsrN undergoes endonucleolytic processing; cyan lines indicate the 5' end of GsrN and pink lines indicate the 3' end of GsrN (post-processing). Pink arrows refer to residues 10 and 50 in the sequence of GsrN, which are deleted from strain *gsrN*(Δ5'). Cyan arrow marks the 5' end of GsrN construct, *gsrN*(Δ3'). Blue highlighted bases in the C-rich loop of GsrN were replaced in the mutant, *gsrN*(RS). (B) Hyperosmotic stress survival assay of *Caulobacter* wild type (WT) and *gsrN* mutant strains. Strains were treated with 300 mM sucrose for 5 hours in a rolling incubator, titered, and plated at 30°C, and colony forming units (CFUs) were enumerated. Plate presented is representative of triplicate assays. Quantification of CFUs in treated versus untreated strains are presented in Fig. S1 in supplemental material. (C) Hyperosmotic survival assay of WT and Δ*gsrN* complemented with either *gsrN(RS)* and or wild type *gsrN.* Plate is representative of triplicate assays. Quantification of CFUs in treated versus untreated strains are presented in Fig. S1 in supplemental material.

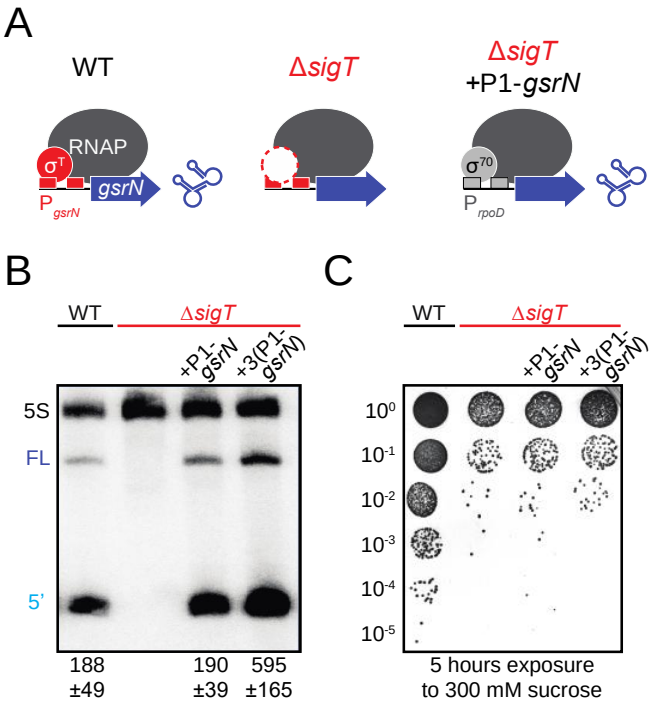

682

683 **FIG 2 *gsrN*-dependent osmotic stress protection requires *sigT***. (A) Schematic of *gsrN* transcription in wild
684 type (WT), Δ*sigT*, and a Δ*sigT* strain bearing the P1-*gsrN* expression system (Δ*sigT*+P1-*gsrN*). P1 is a
685 RpoD(σ^{70})-dependent promoter. (B) Northern blot of total RNA from wild type, Δ*sigT*, Δ*sigT*+P1-*gsrN*, and
686 Δ*sigT*+3(P1-*gsrN*) probed with radiolabeled oligos specific to GsrN and 5S rRNA (loading control). Labels on the
687 left refer to 5S rRNA (5S in black), full-length GsrN (FL in dark blue), and the 5' isoform of GsrN (5' in cyan).
688 Quantified values below the blot are mean ±SD of total normalized signal (FL + 5'), n = 3 independent replicates.
689 (C) Hyperosmotic stress survival assay of wild type (WT) and Δ*sigT* expressing P1-*gsrN* or 3(P1-*gsrN*). Plate is
690 representative of triplicate assays. Quantification of CFUs in treated versus untreated strains are presented in
691 Fig. S1 in supplemental material.

692

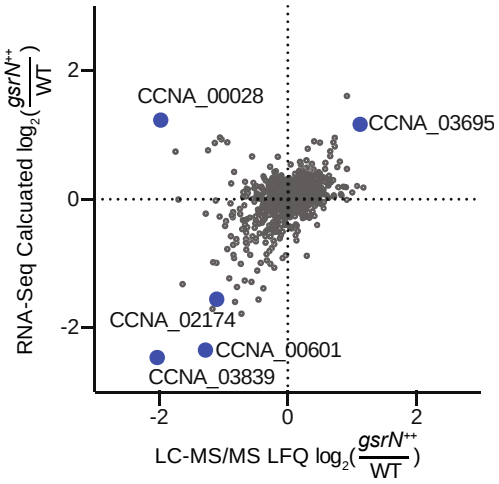

FIG 3 *gsrN*-regulated genes under hyperosmotic conditions. Transcriptomic and proteomic analysis of *gsrN*$^{++}$ and wild type (WT) strains after sucrose-induced hyperosmotic stress. Only genes detected in both analyses are plotted. Blue points indicate genes whose transcript and protein levels differed significantly between *gsrN*$^{++}$ and WT. Significant differential regulation cutoff was log_2(fold) > 1.0 and FDR *p-value* < 0.05 for both transcript and protein based on Wald's Test and Student's t-test, respectively. RNA-Seq data set comprises of 3 wild-type unstressed, 3 wild-type stressed, 4 *gsrN*$^{++}$ unstressed, and 4 *gsrN*$^{++}$ stressed conditions. LC-MS/MS data set comprises the same number of samples for each respective strain and treatment.

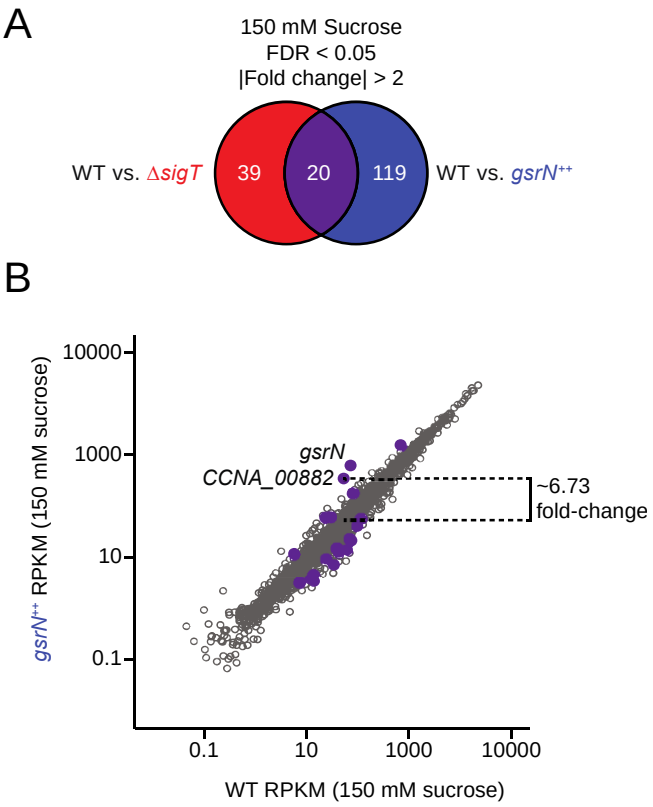

FIG 4 Comparative RNA-seq analysis uncovers candidate targets of GsrN under hyperosmotic stress. (A) RNA-Seq Venn summary of common differentially regulated genes (purple) in wild type (WT) versus Δ*sigT* (red) and WT versus *gsrN*$^{++}$ (blue) during sucrose-induced hyperosmotic stress. Significant differential regulation cutoff was log_2(fold) > 1.0 and FDR *p-value* < 0.05 for both comparisons. (B) Measured transcript abundance, reads per kilobase per million (RPKM) -- log_{10} scale -- of WT and *gsrN*$^{++}$ samples isolated from strains subjected to sucrose-induced hyperosmotic stress. Purple points represent genes identified in (A). Dotted line outlines a 2.75 log_2(fold) change of *CCNA_00882* (*osrP*) between *gsrN*$^{++}$ and WT.

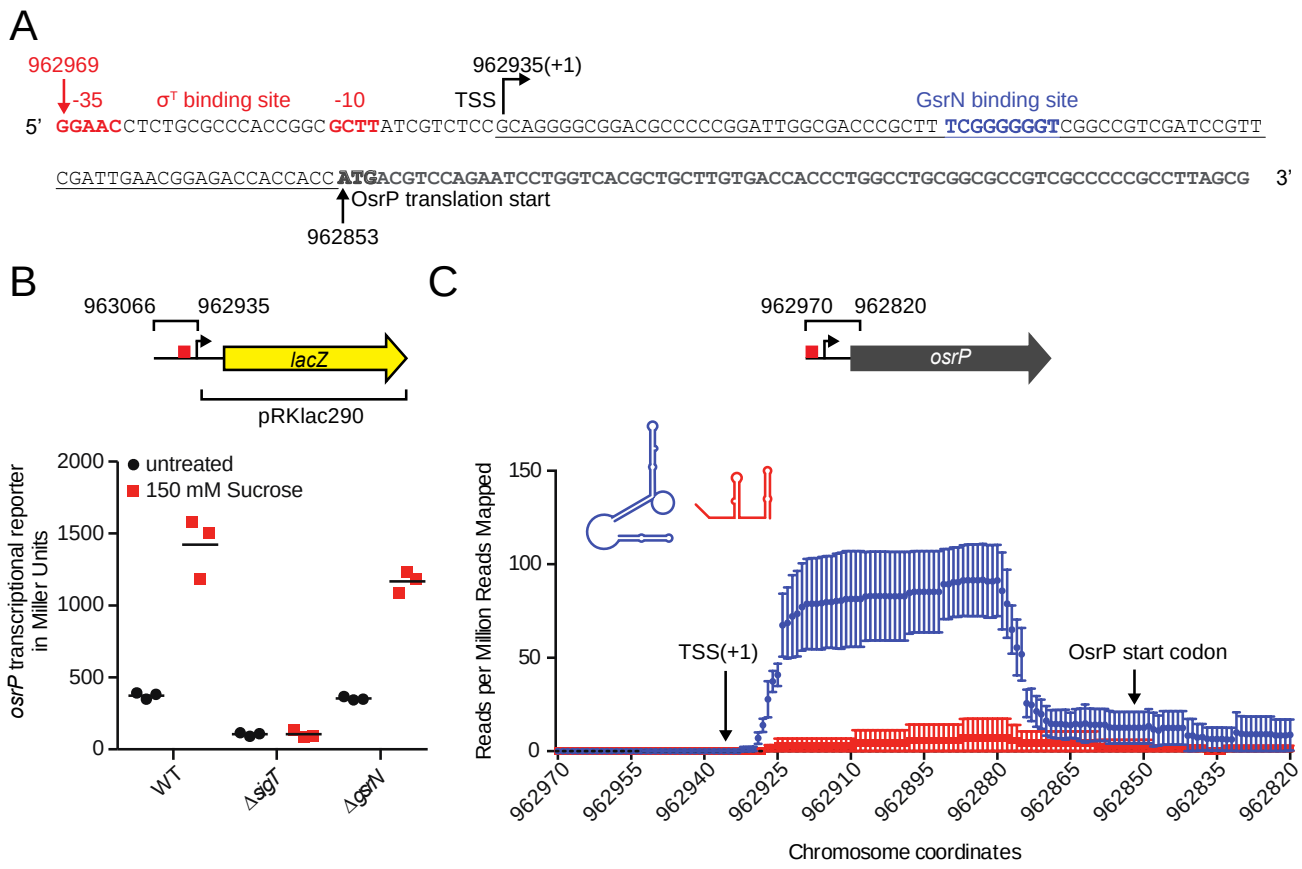

FIG 5 *osrP* is transcribed by σ^T and is upregulated during hyperosmotic stress. (A) *osrP* promoter and leader sequence through the *osrP* translation start site is pictured. Bent arrow indicates the location of the mapped transcriptional start site (TSS) from 5' RACE. Red nucleotides indicate the location of the proposed σ^T-binding site at -10 and -35. Blue nucleotides indicate the proposed GsrN binding site from (11). Black arrow and bolded nucleotides indicate the annotated translation start site of *osrP*. Underlined sequence indicates the region corresponding to the 5' leader of *osrP* mRNA. (B) β-galactosidase activity assay (in Miller Units) of the pRKLac290-*osrP* transcriptional reporter plasmid in wild type (WT), Δ*sigT*, and Δ*gsrN* backgrounds; a schematic of the reporter plasmid marking the cloned region of the *osrP* promoter sequence is pictured above the reporter data. Black circles represent measured activity in log phase cultures. Red squares represent measured activity in cultures treated with 150 mM sucrose for 3 hours. Horizontal bars mark the mean of three independent biological replicates. (C) mRNA that co-purified with *gsrN(37)::PP7hp* (aptamer-tagged GsrN; blue) and *PP7hp::gsrN-3'* (negative control; red) quantified as fractional reads mapped to the leader region of *osrP*. Read density in each dataset represents read coverage at each nucleotide divided by the number of million reads

mapped in that data set. Data represent mean ±SD of three replicate *gsrN(37)::PP7hp* and two replicate *PP7hp::gsrN-3'* purifications.

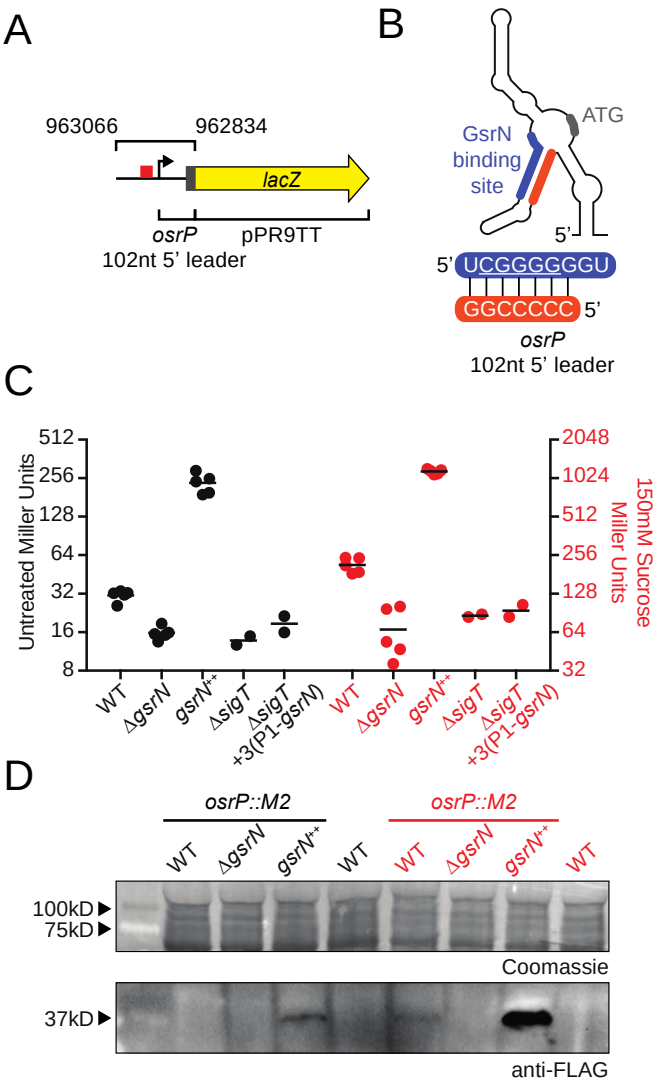

729

730 **FIG 6**. **GsrN activates the expression of OsrP at the post-transcriptional level**. (A) Schematic of the
731 pPR9TT-*osrP* transcription plus translation (TT) reporter plasmid. Top black bracket marks the region of *osrP*
732 (upstream region, 5' UTR, and nucleotides encoding the first 7 amino acids) translationally-fused to *lacZ* in
733 pPR9TT (bottom black bracket). 5' leader of *osrP* (5' UTR and nucleotides encoding the first 7 amino acids) are
734 also identified and comprise 102 bases. (B) Predicted secondary structure (26) of 5' leader of *osrP*. A proposed
735 GsrN binding site is highlighted in blue (see also Fig 5). Base-paired region complementary to the proposed
736 GsrN binding site is highlighted in orange. Start codon is highlighted in grey. Sequence below shows the
737 interaction between the predicted GsrN-binding site and the complementary base-paired region within the 5'
738 leader of *osrP*. (C) β-galactosidase activity assay (in Miller Units) of pPR9TT-*osrP* reporter plasmid in strains
739 listed along the x-axis. Left black axis represents the measured reporter activity of untreated cultures on a log_2
740 scale. Right red axis represents the measured reporter activity in sucrose-treated cultures (outlined in Fig. 5B)

741 on a log_2 scale. Data and mean represent at least two biological replicates. (D) Western analysis of total protein
742 from WT, Δ*gsrN*, and *gsrN*++ strains containing *osrP::M2*, blotted with anti-FLAG. Western blots of cell lysate
743 from untreated (black) and sucrose-treated (red) cultures are shown. Sucrose-treatment to induce hyperosmotic
744 shock was the same as outlined in Fig. 5B. Coomassie-stained membrane (top panel), cut from the blotted
745 bottom panel, is shown as a loading control. Blot presented is overexposed with the majority of the signal in the
746 OsrP::M2 band in the $gsrN^{++}$ treated lane hitting pixel saturation. Arrows on the left indicate size markers from
747 protein ladder. Blot and stained membrane are representative of duplicate experiments.

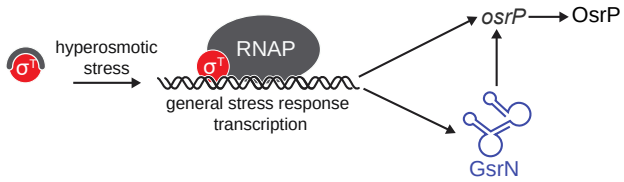

748

749 **FIG 7. Coherent feedforward regulation during hyperosmotic stress in *C. crescentus***. σ^T is de-repressed
750 upon exposure to hyperosmotic stress, and binds to core RNA polymerase (RNAP). σ^T subsequently activates
751 transcription of a set of genes (see Table S3), most notably the sRNA, GsrN. GsrN accumulates in the cell and
752 functions to either activate or repress expression of genes at the post-transcriptional level (see Table S4). *osrP*
753 is among a set of genes in the GSR hyperosmotic stress regulon that are upregulated by σ^T at the
754 transcriptional level and also upregulated by GsrN at the post-transcriptional level, i.e. coherent feedforward
755 regulation.

756

TABLE 1 Proteins with significant differences in steady-state levels between *gsrN*$^{++}$ and wild type (*gsrN*$^{++}$ / WT), with associated transcript changes.

gene name	annotated function	RNA-Seq[a]			LC-MS/MS[b]		
		log$_2$ (Fold)	*p-value*	FDR	*log*$_2$ (Fold)	*p-value*	FDR
CCNA_02831	conserved hypothetical protein	-0.57	0	0.0002	-1.10	0.0001	0.0134
CCNA_03693	creatinine amidohydrolase family protein	0.30	0.0042	0.0516	-1.57	0.0043	0.0488
CCNA_01997	ribosome recycling factor (RRF)	0.26	0.0687	0.3189	-1.20	0.0002	0.0134
CCNA_03852	phosphoribosylformimino-5-aminoimidazole carboxamide ribonucleotide isomerase	0.17	0.0883	0.3601	-1.62	0	0.0093
CCNA_02388	ribose 5-phosphate isomerase	-0.18	0.1314	0.4512	-1.04	0.0002	0.0134
CCNA_01378	protein-L-isoaspartate O-methyltransferase	0.17	0.1427	0.4707	-1.09	0.0005	0.0156
CCNA_03874	carboxymethylenebutenolidase	0.18	0.1805	0.5301	-1.42	0.0008	0.0201
CCNA_03729	transaldolase-like protein	0.18	0.2041	0.5633	-1.39	0	0.0093
CCNA_01327	adenylate kinase/nucleoside-diphosphate kinase Adk	0.15	0.2295	0.5976	-1.93	0.0001	0.0134
CCNA_01586	ABC transporter, ATP-binding protein	1.15	0.2831	0.6632	-1.97	0.0011	0.0232
CCNA_01624	orotate phosphoribosyltransferase	0.14	0.3167	0.6997	-1.21	0.0014	0.0250
CCNA_00045	inorganic pyrophosphatase	0.12	0.3566	0.7311	-1.27	0.0003	0.0155
CCNA_03672	superoxide dismutase	-0.12	0.5448	0.8605	-1.22	0.0002	0.0134
CCNA_01562	4-hydroxy-2-oxoglutarate aldolase/2-dehydro-3-deoxyphosphogluconate aldolase	0.06	0.5595	0.8694	-1.10	0.0003	0.0142
CCNA_01179	3'-phosphoadenosine 5'-phosphosulfate sulfotransferase CysH	-0.08	0.6128	0.8957	-1.12	0.0028	0.0380
CCNA_02741	conserved hypothetical protein	-0.13	0.6809	0.9288	-1.45	0	0.0088
CCNA_01960	acetyl-CoA carboxylase biotin carboxyl carrier protein subunit	-0.04	0.7571	0.9519	-1.94	0.0004	0.0156
CCNA_00545	acetoacetyl-CoA reductase	0.05	0.8240	0.9722	-1.32	0.0004	0.0156
CCNA_01747	3-oxoacyl-(acyl-carrier protein) reductase	0.02	0.8455	0.9775	-1.17	0.0002	0.0134
CCNA_01991	OmpH-like outer membrane protein	0.05	0.8580	0.9800	-1.22	0.0002	0.0134
CCNA_03584	histidine phosphotransferase ChpT	0.02	0.8796	0.9871	-1.40	0.0003	0.0146
CCNA_02293	thiol:disulfide interchange protein TlpA	0.02	0.9070	0.9926	-1.05	0.0005	0.0156

[a]Wald's Test
[b]Student's t-test

762 **TABLE 2** Proteins with significant differences in steady-state levels between *gsrN*$^{++}$ and wild type (*gsrN*$^{++}$ / WT)
763 during hyperosmotic stress, with associated transcript changes.

gene name	annotated function	RNA-Seq[a]			LC-MS/MS[b]		
		log$_2$ (Fold)	*p-value**	FDR*	*log*$_2$ (Fold)	*p-value*	FDR
CCNA_03839	**acylamino-acid-releasing enzyme**	**-2.46**	**0**	**0**	**-2.03**	**0.00027**	**0.01505**
CCNA_00601	**MoxR-like ATPase**	**-2.34**	**0**	**0**	**-1.28**	**0.00058**	**0.02198**
CCNA_02174	**multidrug resistance efflux pump**	**-1.55**	**0**	**0**	**-1.10**	**0.00236**	**0.03647**
CCNA_02540	N-acyl-L-amino acid amidohydrolase	-0.98	0	0	-1.16	0.00057	0.02198
CCNA_00214	TonB-dependent receptor	0.74	6.6e-07	8.5E-06	-1.74	0.00184	0.03167
CCNA_03023	TonB-dependent receptor	0.88	4.38E-09	7.5E-08	-1.13	0.00250	0.03648
CCNA_03157	conserved hypothetical protein	0.96	1.22E-09	2.4E-08	-1.05	0.00421	0.04462
CCNA_03695	**aldehyde dehydrogenase**	**1.17**	**0**	**0**	**1.13**	**0.00465**	**0.04462**
CCNA_00028	**TonB-dependent receptor**	**1.23**	**1.8E-13**	**4.9E-12**	**-1.97**	**0.00066**	**0.02198**

764 [a]Wald's Test
765 [b]Student's t-test
766 * p values and FDR value of zero are < 1e-17
767

768 **Table 3**. RNA-seq analysis of Δ*sigT* and *gsrN*$^{++}$ during hyperosmotic stress.

		***gsrN*$^{++}$/WT**			**Δ*sigT*/WT**		
gene name	**annotated function**	***log*$_2$ (Fold)**	***p-value*[1]**	**FDR[1]**	***log*$_2$ (Fold)**	***p-value*[1]**	**FDR[1]**
gsrN	cell cycle regulated sRNA gsrN	3.14	0	0	-6.27	7.98E-14	3.33E-12
CCNA_00882	hypothetical protein	2.75	0	0	-5.82	0	0
CCNA_03694	AcoR-family transcriptional regulator	1.37	0	0	-1.64	0	0
CCNA_00028*	TonB-dependent receptor	1.23	1.82E-13	4.90E-12	-1.32	2.85E-14	1.27E-12
CCNA_03695*	aldehyde dehydrogenase	1.17	0	0	-1.40	1.10E-05	1.52E-04
CCNA_03889	conserved hypothetical protein	1.10	1.55E-04	1.25E-03	-1.30	1.92E-12	7.13E-11
CCNA_00709	hypothetical protein	1.07	5.67E-04	3.89E-03	-6.22	3.90E-06	5.97E-05
CCNA_01089	conserved hypothetical protein	-1.00	1.11E-16	4.12E-15	1.18	5.44E-13	2.10E-11
CCNA_02051	imidazolonepropionase related amidohydrolase	-1.22	0	0	1.11	3.09E-09	7.70E-08
CCNA_01653	cyclophilin-type peptidylprolyl cis-trans isomerase	-1.23	0	0	1.39	0	0
CCNA_00243	hypothetical protein	-1.33	0	0	1.25	3.13E-11	9.84E-10
CCNA_03082	hypothetical protein	-1.34	0	0	1.24	2.82E-12	1.03E-10
CCNA_01100	acylamino-acid-releasing enzyme	-1.55	0	0	1.16	9.52E-10	2.56E-08
CCNA_02174*	multidrug resistance efflux pump	-1.55	0	0	2.32	0	0
CCNA_02935	methyl-accepting chemotaxis protein	-1.66	0	0	2.12	0	0
CCNA_02172	ABC-type transporter, permease component	-1.72	0	0	2.37	0	0
CCNA_02173	ABC transporter ATP-binding protein	-1.79	0	0	2.29	0	0
CCNA_01247	CESA-like glycosyltransferase	-2.00	0	0	-1.53	6.29E-10	1.72E-08
CCNA_02050	imidazolonepropionase related amidohydrolase	-2.10	0	0	1.29	2.91E-08	6.51E-07
CCNA_03687	carbonic anhydrase	-2.24	0	0	1.99	0	0

769 *Genes also identified in Fig. 3
770 [1] p values and FDR value of zero are < 1e-17

References

1. **Hoch JA, Silhavy TJ.** 1995. Two-Component Signal Transduction. ASM Press, Washington, D.C.
2. **Helmann JD.** 2002. The extracytoplasmic function (ECF) sigma factors. Adv Microb Physiol **46:**47-110.
3. **Paget MS.** 2015. Bacterial Sigma Factors and Anti-Sigma Factors: Structure, Function and Distribution. Biomolecules **5:**1245-1265.
4. **Bastiat B, Sauviac L, Bruand C.** 2010. Dual control of Sinorhizobium meliloti RpoE2 sigma factor activity by two PhyR-type two-component response regulators. J Bacteriol **192:**2255-2265.
5. **Francez-Charlot A, Frunzke J, Reichen C, Ebneter JZ, Gourion B, Vorholt JA.** 2009. Sigma factor mimicry involved in regulation of general stress response. Proc Natl Acad Sci U S A **106:**3467-3472.
6. **Herrou J, Foreman R, Fiebig A, Crosson S.** 2010. A structural model of anti-anti-sigma inhibition by a two-component receiver domain: the PhyR stress response regulator. Mol Microbiol **78:**290-304.
7. **Lourenco RF, Kohler C, Gomes SL.** 2011. A two-component system, an anti-sigma factor and two paralogous ECF sigma factors are involved in the control of general stress response in Caulobacter crescentus. Mol Microbiol **80:**1598-1612.
8. **Fiebig A, Herrou J, Willett J, Crosson S.** 2015. General Stress Signaling in the Alphaproteobacteria. Annu Rev Genet **49:**603-625.
9. **Francez-Charlot A, Kaczmarczyk A, Fischer HM, Vorholt JA.** 2015. The general stress response in Alphaproteobacteria. Trends Microbiol **23:**164-171.
10. **Tien MZ.** 2017. Iterative Rank, GitHub, https://github.com/mtien/IterativeRank.
11. **Tien M, Fiebig A, Crosson S.** 2018. Gene network analysis identifies a central post-transcriptional regulator of cellular stress survival. Elife **7:**e33684.
12. **Andersen J, Forst SA, Zhao K, Inouye M, Delihas N.** 1989. The function of micF RNA. micF RNA is a major factor in the thermal regulation of OmpF protein in Escherichia coli. J Biol Chem **264:**17961-17970.
13. **Bojanovic K, D'Arrigo I, Long KS.** 2017. Global Transcriptional Responses to Osmotic, Oxidative, and Imipenem Stress Conditions in Pseudomonas putida. Appl Environ Microbiol **83:**e03236-03216.
14. **Gomez-Lozano M, Marvig RL, Tulstrup MV, Molin S.** 2014. Expression of antisense small RNAs in response to stress in Pseudomonas aeruginosa. BMC Genomics **15:**783.
15. **Majdalani N, Chen S, Murrow J, St John K, Gottesman S.** 2001. Regulation of RpoS by a novel small RNA: the characterization of RprA. Mol Microbiol **39:**1382-1394.
16. **Guillier M, Gottesman S.** 2006. Remodelling of the Escherichia coli outer membrane by two small regulatory RNAs. Mol Microbiol **59:**231-247.
17. **Chen S, Zhang A, Blyn LB, Storz G.** 2004. MicC, a second small-RNA regulator of Omp protein expression in Escherichia coli. J Bacteriol **186:**6689-6697.
18. **Guillier M, Gottesman S.** 2008. The 5' end of two redundant sRNAs is involved in the regulation of multiple targets, including their own regulator. Nucleic Acids Res **36:**6781-6794.
19. **Kim S, Jeon TJ, Oberai A, Yang D, Schmidt JJ, Bowie JU.** 2005. Transmembrane glycine zippers: physiological and pathological roles in membrane proteins. Proc Natl Acad Sci U S A **102:**14278-14283.
20. **Foreman R, Fiebig A, Crosson S.** 2012. The LovK-LovR two-component system is a regulator of the general stress pathway in Caulobacter crescentus. J Bacteriol **194:**3038-3049.
21. **Alvarez-Martinez CE, Lourenco RF, Baldini RL, Laub MT, Gomes SL.** 2007. The ECF sigma factor sigma(T) is involved in osmotic and oxidative stress responses in Caulobacter crescentus. Mol Microbiol **66:**1240-1255.
22. **Altschul SF, Gish W, Miller W, Myers EW, Lipman DJ.** 1990. Basic local alignment search tool. J Mol Biol **215:**403-410.

23. **Nielsen H.** 2017. Predicting Secretory Proteins with SignalP. Methods Mol Biol **1611:**59-73.
24. **Mann M, Wright PR, Backofen R.** 2017. IntaRNA 2.0: enhanced and customizable prediction of RNA-RNA interactions. Nucleic Acids Res **45:**W435-W439.
25. **Zuker M.** 2003. Mfold web server for nucleic acid folding and hybridization prediction. Nucleic Acids Res **31:**3406-3415.
26. **Mathews DH, Turner DH, Zuker M.** 2007. RNA secondary structure prediction. Curr Protoc Nucleic Acid Chem **Chapter 11:**Unit 11 12.
27. **Kempf B, Bremer E.** 1998. Uptake and synthesis of compatible solutes as microbial stress responses to high-osmolality environments. Arch Microbiol **170:**319-330.
28. **Alon U.** 2007. Network motifs: theory and experimental approaches. Nat Rev Genet **8:**450-461.
29. **Beisel CL, Storz G.** 2011. The base-pairing RNA spot 42 participates in a multioutput feedforward loop to help enact catabolite repression in Escherichia coli. Mol Cell **41:**286-297.
30. **Papenfort K, Espinosa E, Casadesus J, Vogel J.** 2015. Small RNA-based feedforward loop with AND-gate logic regulates extrachromosomal DNA transfer in Salmonella. Proc Natl Acad Sci U S A **112:**E4772-4781.
31. **Plumbridge J, Bossi L, Oberto J, Wade JT, Figueroa-Bossi N.** 2014. Interplay of transcriptional and small RNA-dependent control mechanisms regulates chitosugar uptake in Escherichia coli and Salmonella. Mol Microbiol **92:**648-658.
32. **Majdalani N, Gottesman S.** 2005. The Rcs phosphorelay: a complex signal transduction system. Annu Rev Microbiol **59:**379-405.
33. **Cover TL, Blanke SR.** 2005. Helicobacter pylori VacA, a paradigm for toxin multifunctionality. Nat Rev Microbiol **3:**320-332.
34. **Price MN, Wetmore KM, Waters RJ, Callaghan M, Ray J, Liu H, Kuehl JV, Melnyk RA, Lamson JS, Suh Y, Carlson HK, Esquivel Z, Sadeeshkumar H, Chakraborty R, Zane GM, Rubin BE, Wall JD, Visel A, Bristow J, Blow MJ, Arkin AP, Deutschbauer AM.** 2018. Mutant phenotypes for thousands of bacterial genes of unknown function. Nature **557:**503-509.
35. **Biondi EG, Reisinger SJ, Skerker JM, Arif M, Perchuk BS, Ryan KR, Laub MT.** 2006. Regulation of the bacterial cell cycle by an integrated genetic circuit. Nature **444:**899-904.
36. **Britos L, Abeliuk E, Taverner T, Lipton M, McAdams H, Shapiro L.** 2011. Regulatory response to carbon starvation in Caulobacter crescentus. PLoS One **6:**e18179.
37. **Gogol EB, Rhodius VA, Papenfort K, Vogel J, Gross CA.** 2011. Small RNAs endow a transcriptional activator with essential repressor functions for single-tier control of a global stress regulon. Proc Natl Acad Sci U S A **108:**12875-12880.
38. **Poindexter JS.** 1964. Biological Properties and Classification of the Caulobacter Group. Bacteriol Rev **28:**231-295.
39. **Ely B.** 1991. Genetics of Caulobacter crescentus. Methods Enzymol **204:**372-384.
40. **Finan TM, Kunkel B, De Vos GF, Signer ER.** 1986. Second symbiotic megaplasmid in Rhizobium meliloti carrying exopolysaccharide and thiamine synthesis genes. J Bacteriol **167:**66-72.
41. **Thanbichler M, Iniesta AA, Shapiro L.** 2007. A comprehensive set of plasmids for vanillate- and xylose-inducible gene expression in Caulobacter crescentus. Nucleic Acids Res **35:**e137.
42. **Ried JL, Collmer A.** 1987. An nptI-sacB-sacR cartridge for constructing directed, unmarked mutations in gram-negative bacteria by marker exchange-eviction mutagenesis. Gene **57:**239-246.
43. **West L, Yang D, Stephens C.** 2002. Use of the Caulobacter crescentus genome sequence to develop a method for systematic genetic mapping. J Bacteriol **184:**2155-2166.
44. **Santos PM, Di Bartolo I, Blatny JM, Zennaro E, Valla S.** 2001. New broad-host-range promoter probe vectors based on the plasmid RK2 replicon. FEMS Microbiol Lett **195:**91-96.
45. **Marks ME, Castro-Rojas CM, Teiling C, Du L, Kapatral V, Walunas TL, Crosson S.** 2010. The genetic basis of laboratory adaptation in Caulobacter crescentus. J Bacteriol **192:**3678-3688.

46. **Truman AW, Kristjansdottir K, Wolfgeher D, Hasin N, Polier S, Zhang H, Perrett S, Prodromou C, Jones GW, Kron SJ.** 2012. CDK-dependent Hsp70 Phosphorylation controls G1 cyclin abundance and cell-cycle progression. Cell **151:**1308-1318.
47. **Cox J, Hein MY, Luber CA, Paron I, Nagaraj N, Mann M.** 2014. Accurate proteome-wide label-free quantification by delayed normalization and maximal peptide ratio extraction, termed MaxLFQ. Mol Cell Proteomics **13:**2513-2526.
48. **Dam P, Olman V, Harris K, Su Z, Xu Y.** 2007. Operon prediction using both genome-specific and general genomic information. Nucleic Acids Res **35:**288-298.
49. **Mao F, Dam P, Chou J, Olman V, Xu Y.** 2009. DOOR: a database for prokaryotic operons. Nucleic Acids Res **37:**D459-463.